



Brief paper

Global trajectory tracking control of VTOL-UAVs without linear velocity measurements[☆]

Abdelkader Abdessameud^a, Abdelhamid Tayebi^{a,b,*}

^a Department of Electrical and Computer Engineering, University of Western Ontario, London, Ontario, Canada, N6A 3K7

^b Department of Electrical Engineering, Lakehead University, Thunder Bay, Ontario, Canada P7B 5E1

ARTICLE INFO

Article history:

Received 17 April 2009

Received in revised form

8 February 2010

Accepted 24 February 2010

Available online 8 April 2010

Keywords:

Trajectory tracking

Unmanned Aerial Vehicles

Linear-velocity observer

ABSTRACT

This paper deals with the position control of Vertical Take-Off and Landing (VTOL) Unmanned Aerial Vehicles (UAVs) without linear velocity measurements. We propose a multistage constructive procedure, exploiting the cascade property of the translational and rotational dynamics. More precisely, we consider the force as a virtual control input for the translational dynamics, from which we extract the required (desired) system attitude and thrust achieving the tracking objective. Thereafter, the control torque is designed to drive the actual attitude to the desired one. A nonlinear observer, as well as some instrumental auxiliary variables are used to obviate the need for the linear velocity. Global asymptotic stability of the overall closed loop system is achieved. Simulation results are provided to show the effectiveness of the proposed control scheme.

© 2010 Elsevier Ltd. All rights reserved.

1. Introduction

The control of Unmanned Aerial Vehicles (UAV) has recently received an increasing interest in the control community. This interest is motivated by their potential applications in areas such as surveillance, search and rescue missions, monuments inspections, etc. VTOL-UAVs, which are suitable for a broad range of applications requiring stationary flights, constitute an important class of thrust propelled UAVs. These vehicles are generally *under-actuated*, i.e., equipped with fewer actuators than degrees-of-freedom. It is clear that one of most important components for reliable autonomous flights is an efficient attitude control and stabilization scheme. In fact, this problem has been the focus of extended research over the past years, resulting in a myriad of successful attitude controllers, see for instance, [Tayebi \(2008\)](#) and [Wen and Kreutz-Delgado \(1991\)](#). However, the position control of under-actuated VTOL vehicles in $SE(3)$ is more challenging than the attitude control problem since global asymptotic stability is difficult to achieve for this class of mechanical systems. Several solutions have been reported in the literature, such as the feedback

linearization method in [Koo and Sastry \(1998\)](#), the backstepping approach in [Frazzoli, Dahleh, and Feron \(2000\)](#) and [Pflimlin, Soueres, and Hamel \(2007\)](#), the sliding mode technique in [Madani and Benallegue \(2007\)](#), and other control strategies based on gain scheduling ([Kaminer, Pascoal, Hallberg, & Silvestre, 1998](#)) or on a nested saturation technique ([Kendoul, Lara, Fantoni, & Lozano, 2006](#)).

The authors in [Hamel, Mahony, Lozano, and Ostrowski \(2002\)](#) and [Pflimlin et al. \(2007\)](#) proposed a hierarchical design procedure for the position control of VTOL-UAVs. The idea consists in using the vehicle's orientation and the thrust as control variables to stabilize the vehicle's position, and then apply a classical backstepping procedure to determine the torque-input capable of stabilizing the required orientation. In [Hua, Hamel, Morin, and Samson \(2009\)](#), a similar control architecture is applied to solve the trajectory tracking problem, where the angular velocity is used as an intermediate variable instead of the orientation. The authors in [Aguilar and Hespanha \(2007\)](#) proposed a backstepping design for the trajectory tracking problem of a class of under-actuated systems, including VTOL vehicles, where the states are guaranteed to converge to a ball near the origin.

While the above control schemes rely on the availability of the full state for feedback, only few work has been done in the case where the linear velocity is not available for feedback. For flying vehicles, velocity estimations can be obtained via approximate derivation of the successive measurements from GPS sensors. For fast moving vehicles, the standard procedure consists of integrating the acceleration, and coupling this result with the derivative of the GPS measurements ([Benzemrane, Santosuosso, & Damm, 2007](#)). This estimation method suffers from several

[☆] The material in this paper was not presented at any conference. This paper was recommended for publication in revised form by Associate Editor Yong-Yan Cao under the direction of Editor Toshiharu Sugie.

* Corresponding author at: Department of Electrical and Computer Engineering, University of Western Ontario, London, Ontario, Canada, N6A 3K7. Tel.: +1 807 343 8597; fax: +1 807 766 7243.

E-mail addresses: aabdessa@uwo.ca (A. Abdessameud), tayebi@ieee.org (A. Tayebi).

problems, namely the fact that the errors induced by a GPS system may reach many meters, and in practice, numerical integration along with measurement noise induces a very fast growing velocity measurement error. There are several technical solutions to overcome these problems such as using high-precision sensors like a D-GPS. However, the GPS signal is not available in indoor and urban applications (structure/bridge inspection for example) due to signal blockage and attenuation, which may deteriorate the positioning accuracy. To solve the linear-velocity estimation problem without the use of a GPS, several authors have considered the combination of artificial vision and the inertial sensors, see for example Cheviron, Hamel, Mahony, and Baldwin (2007), Rondon, Salazar, Escareno, and Lozano (2010) and references therein. Another solution is to use observers to estimate the missing states, as done in Do, Jiang, and Pan (2003), where the trajectory tracking problem of a *planar*-VTOL is treated. It is worth mentioning, that in the case where a GPS is not available (in indoor applications for instance), there are several techniques that allow to obtain the UAV position, such as the combination of an inertial measurement unit (IMU) with a vision system; or the use of a network of Ultra-wideband (UWB) receivers which track a large number of small (inexpensive) UWB transmitters.

The main contribution of this work is to provide a solution to the position tracking problem of VTOL UAVs without linear-velocity measurements. We exploit the cascaded nature of the system and first design an *intermediary* control input for the translational dynamics of the vehicle, without linear velocity measurements, from which we can *extract* the magnitude of the necessary thrust input and the desired orientation (in terms of unit-quaternion) of the aircraft. The thrust input will be used to drive the translational dynamics of the aircraft, and the time-varying desired attitude will be considered as a reference input to be tracked by the rotational dynamics with an appropriate design of the torque input.

In our approach, we ensure that the intermediary translational control input is *a priori* bounded and at least twice differentiable. This, as it will become clear later, will be a key ingredient guaranteeing the existence of a solution to the attitude and thrust extraction algorithm, as well as the boundedness of the actual control inputs. As a result, the proposed control scheme guarantees global asymptotic trajectory tracking with an *a priori* bounded thrust.

2. System model

In this paper, we consider a VTOL aircraft modeled as a rigid-body. Let $\mathcal{F}_i \triangleq \{\hat{\mathbf{e}}_1, \hat{\mathbf{e}}_2, \hat{\mathbf{e}}_3\}$ denotes the inertial frame, and $\mathcal{F}_b \triangleq \{\hat{\mathbf{e}}_{1b}, \hat{\mathbf{e}}_{2b}, \hat{\mathbf{e}}_{3b}\}$ denotes the body-fixed frame of the aircraft. Let the position and linear velocity of the aircraft, expressed in the inertial frame \mathcal{F}_i , be denoted by $\mathbf{p} \in \mathbb{R}^3$ and $\mathbf{v} \in \mathbb{R}^3$ respectively, and let its angular velocity, expressed in the body-fixed frame \mathcal{F}_b , be denoted by $\boldsymbol{\omega} \in \mathbb{R}^3$. To represent the attitude (orientation) of the aircraft, we make use of the unit-quaternion representation (Shuster, 1993). The unit-quaternion $\mathbf{Q} = (\mathbf{q}^T, \eta)^T$ is a four-element vector, composed of a vector component $\mathbf{q} \in \mathbb{R}^3$ and a scalar component $\eta \in \mathbb{R}$, satisfying the unity constraint: $\mathbf{q}^T \mathbf{q} + \eta^2 = 1$. The orthogonal rotation matrix $\mathbf{R}(\mathbf{Q}) \in SO(3)$ that defines the rotation of the body frame by an angle γ about the axis described by the unit vector $\hat{\mathbf{k}} \in \mathbb{R}^3$, can be described by a unit-quaternion $\mathbf{Q} = (\mathbf{q}^T, \eta)^T$ such that: $\mathbf{q} = \hat{\mathbf{k}} \sin(\gamma/2)$, and $\eta = \cos(\gamma/2)$. The rotation matrix $\mathbf{R}(\mathbf{Q})$, related to the unit-quaternion \mathbf{Q} , that brings the inertial frame into the body frame, can be obtained through the Rodriguez formula as: $\mathbf{R}(\mathbf{Q}) = (\eta^2 - \mathbf{q}^T \mathbf{q}) \mathbf{I}_3 + 2\mathbf{q} \mathbf{q}^T - 2\eta \mathbf{S}(\mathbf{q})$, where \mathbf{I}_3 is the 3-by-3 identity matrix and the matrix $\mathbf{S}(\mathbf{x})$ is the skew-symmetric matrix such that $\mathbf{S}(\mathbf{x})\mathbf{u} = \mathbf{x} \times \mathbf{u}$ for any vector $\mathbf{u} \in \mathbb{R}^3$, where ' \times ' denotes the vector cross product.

The quaternion multiplication between two unit quaternion, $\mathbf{Q}_1 = (\mathbf{q}_1^T, \eta_1)^T$ and $\mathbf{Q}_2 = (\mathbf{q}_2^T, \eta_2)^T$, is defined

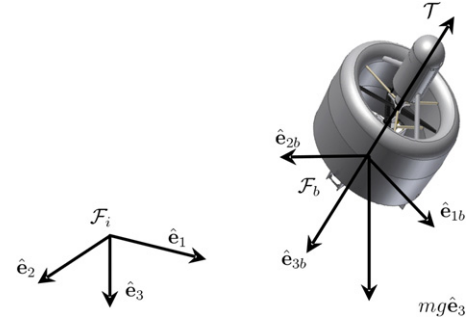


Fig. 1. VTOL aircraft.

by the following non-commutative operation: $\mathbf{Q}_1 \odot \mathbf{Q}_2 = ((\eta_1 \mathbf{q}_2 + \eta_2 \mathbf{q}_1 + \mathbf{S}(\mathbf{q}_1) \mathbf{q}_2)^T, \eta_1 \eta_2 - \mathbf{q}_1^T \mathbf{q}_2)^T$. The inverse or conjugate of a unit quaternion is defined by, $\mathbf{Q}^{-1} = (-\mathbf{q}^T, \eta)^T$, with the quaternion identity given by $(0, 0, 0, 1)^T$, (Shuster, 1993).

Using this representation of the attitude, the equations of motion of the VTOL aircraft can be described by

$$\begin{cases} (\Sigma_1): \begin{cases} \dot{\mathbf{p}} = \mathbf{v}, \\ \dot{\mathbf{v}} = g \hat{\mathbf{e}}_3 - \frac{\mathcal{T}}{m} \mathbf{R}(\mathbf{Q})^T \hat{\mathbf{e}}_3, \end{cases} \\ (\Sigma_2): \begin{cases} \dot{\mathbf{Q}} = \frac{1}{2} \begin{pmatrix} \eta \mathbf{I}_3 + \mathbf{S}(\mathbf{q}) \\ -\mathbf{q}^T \end{pmatrix} \boldsymbol{\omega}, \\ \mathbf{I}_f \dot{\boldsymbol{\omega}} = \boldsymbol{\tau} - \mathbf{S}(\boldsymbol{\omega}) \mathbf{I}_f \boldsymbol{\omega}, \end{cases} \end{cases} \quad (1)$$

where m and g are the aircraft mass and the gravitational acceleration. $\mathbf{I}_f \in \mathbb{R}^{3 \times 3}$ is a symmetric positive definite constant inertia matrix of the vehicle with respect to \mathcal{F}_b . The scalar \mathcal{T} and the vector $\boldsymbol{\tau}$ represent respectively the magnitude of the thrust applied to the vehicle in the direction of $\hat{\mathbf{e}}_{3b}$, and the external torque applied to the system expressed in \mathcal{F}_b . An example of a VTOL aircraft considered in this paper is illustrated in Fig. 1.

3. Problem formulation

Our objective in this work is to design global control laws for the thrust $\mathcal{T}(t)$ and the torque $\boldsymbol{\tau}(t)$ allowing the VTOL aircraft to track a desired trajectory $\mathbf{p}_d(t)$. We assume that the linear-velocity vector is not available for feedback. In other words, we would like to design a linear-velocity-free global control law guaranteeing the boundedness and the asymptotic convergence to zero of the following position and linear-velocity tracking errors

$$\mathbf{e}(t) = \mathbf{p}(t) - \mathbf{p}_d(t), \quad \tilde{\mathbf{v}}(t) \triangleq \dot{\mathbf{e}}(t) = \mathbf{v}(t) - \dot{\mathbf{p}}_d(t). \quad (2)$$

Due to the under-actuated nature of the system, the design of the thrust and torque inputs for this class of systems is not straightforward. In the following, we will present the control design methodology that we adopt in this work to achieve our objectives.

3.1. Thrust and desired attitude extraction

Consider the translational dynamics (Σ_1) in (1), which can be rewritten as

$$(\Sigma_1): \begin{cases} \dot{\mathbf{p}} = \mathbf{v}, \\ \dot{\mathbf{v}} = \mathbf{F} - \frac{\mathcal{T}}{m} f(\mathbf{Q}, \mathbf{Q}_d), \end{cases} \quad (3)$$

with

$$f(\mathbf{Q}, \mathbf{Q}_d) \triangleq (\mathbf{R}(\mathbf{Q})^T - \mathbf{R}(\mathbf{Q}_d)^T) \hat{\mathbf{e}}_3, \quad (4)$$

$$\mathbf{F} \triangleq g \hat{\mathbf{e}}_3 - \frac{\mathcal{T}}{m} \mathbf{R}(\mathbf{Q}_d)^T \hat{\mathbf{e}}_3, \quad (5)$$

where the variable \mathbf{F} is an “intermediary” control input to the translational dynamics, and $\mathbf{Q}_d(t) = (\mathbf{q}_d^T, \eta_d)^T$ is the unit quaternion representing the desired attitude of the vehicle.

In the following Lemma, (Roberts & Tayebi, 2009), we will present a thrust and desired attitude extraction algorithm (in terms of the unit-quaternion) from the expression of the intermediary control input, given in (5).

Lemma 1. Consider Eq. (5) and let the vector $\mathbf{F} \triangleq (\mu_1, \mu_2, \mu_3)^T$. It is always possible to extract the thrust magnitude and the desired system’s attitude from (5) as

$$\mathcal{T} = m\|\mathbf{g}\hat{\mathbf{e}}_3 - \mathbf{F}\|, \quad (6)$$

$$\eta_d = \sqrt{\frac{1}{2} + \frac{m(g - \mu_3)}{2\mathcal{T}}}, \quad \mathbf{q}_d = \frac{m}{2\mathcal{T}\eta_d} \begin{pmatrix} \mu_2 \\ -\mu_1 \\ 0 \end{pmatrix}, \quad (7)$$

under the condition that

$$\mathbf{F} \neq (0, 0, x), \quad \text{for } x \geq g, \quad (8)$$

where $\|\cdot\|$ denotes the Euclidean norm of a vector. In addition, under the condition that the intermediary control \mathbf{F} is differentiable, we can write the desired angular velocity of the aircraft as

$$\boldsymbol{\omega}_d = \boldsymbol{\Xi}(\mathbf{F})\dot{\mathbf{F}}, \quad (9)$$

$$\boldsymbol{\Xi}(\mathbf{F}) = \frac{1}{\gamma_1^2 \gamma_2} \begin{pmatrix} -\mu_1 \mu_2 & -\mu_2^2 + \gamma_1 \gamma_2 & \mu_2 \gamma_2 \\ \mu_1^2 - \gamma_1 \gamma_2 & \mu_1 \mu_2 & -\mu_1 \gamma_2 \\ \mu_2 \gamma_1 & -\mu_1 \gamma_1 & 0 \end{pmatrix}, \quad (10)$$

with $\gamma_1 = (\mathcal{T}/m)$ and $\gamma_2 = \gamma_1 + (g - \mu_3)$.

Proof. A similar proof can be found in Abdessameud and Tayebi (2009) and Roberts and Tayebi (2009). \square

The result in Lemma 1 states that if one is able to design an appropriate intermediary control input $\mathbf{F}(t)$ for the translational dynamics, that satisfies condition (8) for all $t > 0$, then the positive thrust magnitude $\mathcal{T}(t)$, and the aircraft desired attitude $\mathbf{Q}_d(t)$, can be extracted as in (6) and (7) respectively. Note that the solution (6) and (7) is singularity-free.

3.2. Attitude error dynamics

Provided that the aircraft desired attitude \mathbf{Q}_d is determined, we define the attitude tracking error, describing the discrepancy between the vehicle’s attitude and its desired attitude, namely $\tilde{\mathbf{Q}} = (\tilde{\mathbf{q}}^T, \tilde{\eta})^T$, by

$$\tilde{\mathbf{Q}} = \mathbf{Q}_d^{-1} \circ \mathbf{Q}, \quad (11)$$

governed by the unit-quaternion dynamics

$$\dot{\tilde{\mathbf{q}}} = \frac{1}{2}(\tilde{\eta}\mathbf{I}_3 + \mathbf{S}(\tilde{\mathbf{q}}))\tilde{\boldsymbol{\omega}}, \quad \dot{\tilde{\eta}} = -\frac{1}{2}\tilde{\mathbf{q}}^T \tilde{\boldsymbol{\omega}}, \quad (12)$$

$$\dot{\tilde{\boldsymbol{\omega}}} = \boldsymbol{\omega} - \mathbf{R}(\tilde{\mathbf{Q}})\boldsymbol{\omega}_d, \quad (13)$$

where $\tilde{\boldsymbol{\omega}}$ is the angular velocity error vector and $\boldsymbol{\omega}_d$ is the desired angular velocity of the aircraft given in (9). Matrix $\mathbf{R}(\tilde{\mathbf{Q}})$ is the rotation matrix related to $\tilde{\mathbf{Q}}$, and is given by $\mathbf{R}(\tilde{\mathbf{Q}}) = \mathbf{R}(\mathbf{Q})\mathbf{R}(\mathbf{Q}_d)^T$, (Shuster, 1993). With the above definition, we can see that attitude tracking is achieved when $\tilde{\mathbf{Q}}$ coincides with \mathbf{Q}^d , or $\tilde{\mathbf{Q}} = (\mathbf{0}_3^T, \pm 1)^T$, and $\tilde{\boldsymbol{\omega}} = \mathbf{0}_3$, with $\mathbf{0}_3 = \text{col}[0, 0, 0]$. Note that due to the inherent redundancy of the quaternion representation, \mathbf{Q} and $-\mathbf{Q}$ represent the same physical orientation however, one is rotated 2π relative to the other about an arbitrary axis. Accordingly, $\tilde{\mathbf{Q}} = (\mathbf{0}_3^T, \pm 1)^T$ correspond to the same physical point.

From (11) and the definition of $\mathbf{R}(\mathbf{Q})$, it can be easily shown that the function $f(\mathbf{Q}, \mathbf{Q}_d)$ in (4) can be expressed in terms of the elements of $\tilde{\mathbf{Q}}$ as

$$\begin{aligned} f(\mathbf{Q}, \mathbf{Q}_d) &= \mathbf{R}(\mathbf{Q})^T (\mathbf{I}_3 - \mathbf{R}(\tilde{\mathbf{Q}})) \hat{\mathbf{e}}_3 \\ &= 2\mathbf{R}(\mathbf{Q})^T \mathbf{S}(\tilde{\mathbf{q}})\tilde{\mathbf{q}}, \end{aligned} \quad (14)$$

with $\tilde{\mathbf{q}} = (\tilde{q}_1, \tilde{q}_2, \tilde{q}_3)^T$, $\tilde{\mathbf{q}} = (\tilde{q}_2, -\tilde{q}_1, -\tilde{\eta})^T$. In addition, it is easy to verify that $\|\mathbf{R}(\mathbf{Q})^T \mathbf{S}(\tilde{\mathbf{q}})\| \leq 1$.

4. Control design procedure

Based on the above extraction algorithm, the main idea in our design method is to exploit the cascaded nature of the system (1) and consider a control design procedure that can be summarized in the following points:

- (1) Consider the translational dynamics (Σ_1) in (3), and design the intermediary translational control input, \mathbf{F} , for the aircraft that satisfies condition (8) without linear-velocity measurements. Then, using the extraction algorithm in Lemma 1, we extract the necessary thrust $\mathcal{T}(t)$ and the aircraft desired attitude $\mathbf{Q}_d(t)$. The magnitude of the thrust will be the input to the sub-system (Σ_1).
- (2) Consider the rotational dynamics (Σ_2) in (1), and $\mathbf{Q}_d(t)$ as a time varying desired attitude, and design a linear-velocity-free torque input such that the attitude tracking error $\tilde{\mathbf{q}}(t)$ converges asymptotically to zero.
- (3) Show the global asymptotic stability of the overall system.

4.1. Step 1: intermediary position control design

To design an intermediary control \mathbf{F} for the translational dynamics (3) that achieves our control objectives without linear-velocity measurements, we have to take into consideration some important requirements.

First, it is important to notice that for condition (8) to be satisfied, the third element of the control input \mathbf{F} must be bounded *a priori*. Hence, to use the extraction algorithm described in Lemma 1, it is sufficient to design an *a priori* bounded intermediary control \mathbf{F} . On the other hand, we can see that the term $\frac{\mathcal{T}}{m}f(\mathbf{Q}, \mathbf{Q}_d)$ in (3) constitutes a nonlinear perturbation to the translational dynamics, which is completely unknown at this stage of the control design. Fortunately, we know that $f(\mathbf{Q}, \mathbf{Q}_d)$ is bounded since it is function of orthogonal rotation matrices. In addition, we can see from (6) that the design of an *a priori* bounded intermediary control input is necessary to guarantee a bounded thrust input and hence a bounded perturbation term.

Second, we can notice from the expression of $\boldsymbol{\omega}_d$ in (9) that $\dot{\boldsymbol{\omega}}_d$ is function of $\dot{\mathbf{F}}$. It is clear that to implement a trajectory tracking attitude controller, that necessarily requires the knowledge of $\boldsymbol{\omega}_d(t)$ and $\dot{\boldsymbol{\omega}}_d(t)$, we need to ensure that these signals are bounded. In addition, the intermediary control \mathbf{F} must be at least twice differentiable. Moreover, if a nonlinear observer or a partial state feedback is considered in the design of \mathbf{F} using the position tracking errors, $\tilde{\mathbf{F}}$ and $\dot{\tilde{\mathbf{F}}}$ will necessarily be function of \mathbf{v} and $\dot{\mathbf{v}}$, respectively, which are not available for feedback.

To achieve our objectives, and solve the above problems, we introduce the following new variables

$$\boldsymbol{\xi} = \mathbf{e} - \boldsymbol{\theta}, \quad \mathbf{z} = \dot{\boldsymbol{\xi}} = \tilde{\mathbf{v}} - \dot{\boldsymbol{\theta}}, \quad (15)$$

where $\boldsymbol{\theta} \in \mathbb{R}^3$ is a design variable to be determined later. The translational error dynamics can then be written as

$$\dot{\mathbf{z}} = -\frac{\mathcal{T}}{m}f(\mathbf{Q}, \mathbf{Q}_d) + \mathbf{F} - \ddot{\boldsymbol{\theta}} - \dot{\mathbf{p}}_d. \quad (16)$$

Consider the following positive definite function

$$V_t = \frac{1}{2} (\mathbf{z}^T \mathbf{z} + k_p \boldsymbol{\xi}^T \boldsymbol{\xi} + k_d (\boldsymbol{\xi} - \boldsymbol{\psi})^T (\boldsymbol{\xi} - \boldsymbol{\psi})), \quad (17)$$

where k_p, k_d are strictly positive scalar gains, and the design variable $\boldsymbol{\psi}$ is the output of an auxiliary system which plays the role of an estimator of the linear velocity at this stage of the control design. The time derivative of V_t is given as

$$\begin{aligned} \dot{V}_t = & \mathbf{z}^T \left(-\frac{\mathcal{T}}{m} \mathbf{f}(\mathbf{Q}, \mathbf{Q}_d) + \mathbf{F} - \ddot{\boldsymbol{\theta}} - \dot{\mathbf{p}}_d \right) \\ & + \mathbf{z}^T (k_p \boldsymbol{\xi} + k_d (\boldsymbol{\xi} - \boldsymbol{\psi})) - k_d \dot{\boldsymbol{\psi}}^T (\boldsymbol{\xi} - \boldsymbol{\psi}). \end{aligned} \quad (18)$$

Taking

$$\mathbf{F} - \ddot{\boldsymbol{\theta}} = \ddot{\mathbf{p}}_d - k_p \boldsymbol{\xi} - k_d (\boldsymbol{\xi} - \boldsymbol{\psi}), \quad (19)$$

and using (14), we obtain

$$\dot{V}_t = -\frac{2\mathcal{T}}{m} \mathbf{z}^T \mathbf{R}(\mathbf{Q})^T \mathbf{S}(\bar{\mathbf{q}}) \bar{\mathbf{q}} - k_d \dot{\boldsymbol{\psi}}^T (\boldsymbol{\xi} - \boldsymbol{\psi}). \quad (20)$$

It is clear that with a simple design of $\dot{\boldsymbol{\psi}}$, the last term in the right hand side of (20) can be guaranteed to be negative. In addition, to guarantee the stability result of the overall system, as we will see in the proof of our result, the first term in the right hand side of (20) should be considered in the torque input design.

In view of (19), we propose the linear-velocity-free intermediary control input for the VTOL vehicle, \mathbf{F} , and the auxiliary variable $\boldsymbol{\theta}$ as

$$\mathbf{F} = \ddot{\mathbf{p}}_d - k_{\theta_1} \tanh(\boldsymbol{\theta}) - k_{\theta_2} \tanh(\dot{\boldsymbol{\theta}}), \quad (21)$$

$$\ddot{\boldsymbol{\theta}} = -k_{\theta_1} \tanh(\boldsymbol{\theta}) - k_{\theta_2} \tanh(\dot{\boldsymbol{\theta}}) + k_p \boldsymbol{\xi} + k_d (\boldsymbol{\xi} - \boldsymbol{\psi}), \quad (22)$$

where k_{θ_1} and k_{θ_2} are strictly positive scalar gains, and $\boldsymbol{\theta}(0)$ and $\dot{\boldsymbol{\theta}}(0)$ can be selected arbitrarily.

It is worth noticing that the idea behind the introduction of the new variable $\boldsymbol{\theta}$ is to modify (during the transient) the desired trajectory, and design the control scheme such that $\lim_{t \rightarrow \infty} \boldsymbol{\xi} = \mathbf{0}$ and $\lim_{t \rightarrow \infty} \mathbf{z} = \mathbf{0}$. Once this is achieved, the variable $\boldsymbol{\theta}$ and its time derivative are forced to converge to zero, ensuring hence the tracking of the original desired trajectories. As a result, this variable allows the design of an *a priori* bounded control input, \mathbf{F} , such that

$$\|\mathbf{F}\| \leq \|\ddot{\mathbf{p}}_d\| + \sqrt{3}(k_{\theta_1} + k_{\theta_2}). \quad (23)$$

Before we proceed further in our control design, we need the following assumption on the desired trajectory and the control gains.

Assumption 1. The second, third and fourth time-derivatives of the desired trajectory are bounded. The elements of the desired acceleration vector $\ddot{\mathbf{p}}_d(t) := (\ddot{p}_{d_1}, \ddot{p}_{d_2}, \ddot{p}_{d_3})^T$, and the positive control gains k_{θ_1} and k_{θ_2} should satisfy one of the following conditions:

- (a) $k_{\theta_1} + k_{\theta_2} < \|\ddot{p}_{d_1}(t)\|, \forall t \geq 0$,
- (b) $k_{\theta_1} + k_{\theta_2} < \|\ddot{p}_{d_2}(t)\|, \forall t \geq 0$,
- (c) $\|\ddot{p}_{d_3}(t)\| \leq \alpha, \forall t \geq 0$, and $k_{\theta_1} + k_{\theta_2} \leq g - \alpha$,
- (d) $\|\ddot{\mathbf{p}}_d(t)\| \leq \delta, \forall t \geq 0$, and $k_{\theta_1} + k_{\theta_2} \leq \frac{1}{\sqrt{3}}(g - \delta)$

with $\alpha > 0$ and $0 \leq \delta < g$.

It is straightforward to verify that if one of the above cases is met, condition (8) is satisfied, and the intermediary control \mathbf{F} can be used in the extraction method in Lemma 1. In fact, cases (a) and (b) ensure that $\mu_1 \neq 0$ and $\mu_2 \neq 0$ for all $t \geq 0$ respectively, case (c) is considered such that $\mu_3 < g$ for all $t \geq 0$, and finally, the more restrictive case (d) guarantees that $\|\mathbf{F}\| < g$ for all $t \geq 0$. Since \mathbf{F} is bounded, and if condition (8) is satisfied for all time, the extracted value of the thrust \mathcal{T} , in (6), is guaranteed to be positive and *a priori* bounded as

$$\mathcal{T} \leq m \left(g + \delta_d + \sqrt{3}(k_{\theta_1} + k_{\theta_2}) \right) \triangleq \Lambda, \quad (24)$$

with $\delta_d = \|\ddot{\mathbf{p}}_d(t)\|_\infty$ and Λ a positive constant. Also, the extracted desired attitude of the vehicle, $\mathbf{Q}_d(t)$, is guaranteed to be realizable.

4.2. Step 2: attitude control design

Now, we consider the orientation dynamics and design a torque input for the vehicle that guarantees tracking of the desired attitude $\mathbf{Q}_d(t)$ given in (7). It is important to see that the intermediary control \mathbf{F} in (21) does not depend *explicitly* on the position tracking error. As a result, the desired angular velocity, $\boldsymbol{\omega}_d(t)$, derived in (9), does not depend on the linear-velocity signal. However, the time derivative of the desired angular velocity, $\dot{\boldsymbol{\omega}}_d(t)$, will be given as

$$\dot{\boldsymbol{\omega}}_d = \boldsymbol{\Psi}_1 - \boldsymbol{\Psi}_2 \mathbf{z}, \quad (25)$$

where the vector $\boldsymbol{\Psi}_1$ and matrix $\boldsymbol{\Psi}_2$ are derived in the Appendix for the sake of clarity of presentation. It is clear that $\dot{\boldsymbol{\omega}}_d$ is function of the signal \mathbf{z} which depends explicitly on the linear-velocity of the aircraft. Note that without the introduction of the new variable $\boldsymbol{\theta}$, the use of the position tracking error explicitly in the expression of \mathbf{F} results in $\boldsymbol{\omega}_d$ being function of the linear-velocity and $\dot{\boldsymbol{\omega}}_d$ being function of the linear-acceleration, which will make the control design quite complicated.

To design the attitude tracking torque, we introduce the following variable

$$\boldsymbol{\Omega} = \tilde{\boldsymbol{\omega}} - \boldsymbol{\beta}, \quad (26)$$

with $\tilde{\boldsymbol{\omega}}$ defined in (13) and $\boldsymbol{\beta}$ being a design parameter to be determined later. Exploiting the rotational dynamics (Σ_2) in (1) and expression (25), we can easily show that

$$\mathbf{I}_f \dot{\boldsymbol{\Omega}} = \boldsymbol{\tau} - \mathbf{H}(\cdot) + \boldsymbol{\Gamma} \mathbf{z} - \mathbf{I}_f \dot{\boldsymbol{\beta}}, \quad (27)$$

with: $\mathbf{H}(\cdot) = \mathbf{S}(\boldsymbol{\omega}) \mathbf{I}_f \boldsymbol{\omega} - \mathbf{I}_f \mathbf{S}(\tilde{\boldsymbol{\omega}}) \mathbf{R}(\tilde{\mathbf{Q}}) \boldsymbol{\omega}_d + \mathbf{I}_f \mathbf{R}(\tilde{\mathbf{Q}}) \boldsymbol{\Psi}_1$, $\boldsymbol{\Gamma} = \mathbf{I}_f \mathbf{R}(\tilde{\mathbf{Q}}) \boldsymbol{\Psi}_2$, and $\tilde{\mathbf{Q}}$ is given in (11). Note that the angular velocity error dynamics (27) depend on the vector \mathbf{z} , and hence on the aircraft linear-velocity, which is not available for feedback.

To design a torque input in (27) without linear-velocity measurements, we introduce the following nonlinear observer that generates estimates of the linear-velocity vector, $\hat{\mathbf{z}}$, as

$$\begin{cases} \dot{\hat{\mathbf{z}}} \triangleq \hat{\boldsymbol{\xi}} = \mathbf{v} - L_p \tilde{\boldsymbol{\xi}}, \\ \dot{\hat{\mathbf{v}}} = \boldsymbol{\Phi} + \boldsymbol{\Gamma}^T \boldsymbol{\Omega} - L_v^2 \tilde{\boldsymbol{\xi}}, \end{cases} \quad (28)$$

where L_p and L_v are strictly positive scalar gains, $\tilde{\boldsymbol{\xi}} \triangleq (\hat{\boldsymbol{\xi}} - \boldsymbol{\xi})$ and $\boldsymbol{\Phi} \triangleq \mathbf{F} - \ddot{\boldsymbol{\theta}} - \ddot{\mathbf{p}}_d - \frac{\mathcal{T}}{m} \mathbf{f}(\mathbf{Q}, \mathbf{Q}_d)$. It is important to mention that at this stage of the control design, all the signals required for the observer are well determined, among which are \mathbf{F} , $\dot{\boldsymbol{\theta}}$, \mathbf{Q}_d and $\boldsymbol{\omega}_d$.

Define the observation error vector as, $\tilde{\mathbf{z}} \triangleq \hat{\mathbf{z}} - \mathbf{z}$. Using (16), the observation error dynamics can be written as

$$\dot{\tilde{\mathbf{z}}} = -L_p \tilde{\mathbf{z}} - L_v^2 \tilde{\boldsymbol{\xi}} + \boldsymbol{\Gamma}^T \boldsymbol{\Omega}. \quad (29)$$

To design the necessary torque input, we consider the following positive definite function

$$\begin{aligned} V_a = & \frac{1}{2} (\tilde{\mathbf{z}} + L_v \tilde{\boldsymbol{\xi}})^T (\tilde{\mathbf{z}} + L_v \tilde{\boldsymbol{\xi}}) + \frac{1}{2} L_v L_p \tilde{\boldsymbol{\xi}}^T \tilde{\boldsymbol{\xi}} \\ & + 2k_q (1 - \tilde{\eta}) + \frac{1}{2} \boldsymbol{\Omega}^T \mathbf{I}_f \boldsymbol{\Omega}, \end{aligned} \quad (30)$$

with $k_q > 0$. The time derivative of V_a , using (12), (26), (27) and (29), is given as

$$\begin{aligned} \dot{V}_a = & -(L_p - L_v) \tilde{\mathbf{z}}^T \tilde{\mathbf{z}} - L_v^3 \tilde{\boldsymbol{\xi}}^T \tilde{\boldsymbol{\xi}} + (\tilde{\mathbf{z}} + L_v \tilde{\boldsymbol{\xi}})^T \boldsymbol{\Gamma}^T \boldsymbol{\Omega} + k_q \tilde{\mathbf{q}}^T (\boldsymbol{\Omega} + \boldsymbol{\beta}) \\ & + \boldsymbol{\Omega}^T (\boldsymbol{\tau} - \mathbf{H}(\cdot) + \boldsymbol{\Gamma} \mathbf{z} - \mathbf{I}_f \dot{\boldsymbol{\beta}}). \end{aligned} \quad (31)$$

In view of this last equation, and using the observed states, we propose the following torque input for the rotational dynamics

$$\boldsymbol{\tau} = \mathbf{H}(\cdot) + \mathbf{I}_f \dot{\boldsymbol{\beta}} - k_q \tilde{\mathbf{q}} - k_\Omega \boldsymbol{\Omega} - \boldsymbol{\Gamma} (\hat{\mathbf{z}} + L_v \tilde{\boldsymbol{\xi}}), \quad (32)$$

with $k_\Omega > 0$, to obtain

$$\dot{V}_a = -(L_p - L_v) \tilde{\mathbf{z}}^T \tilde{\mathbf{z}} - L_v^3 \tilde{\boldsymbol{\xi}}^T \tilde{\boldsymbol{\xi}} + k_q \tilde{\mathbf{q}}^T \boldsymbol{\beta} - k_\Omega \boldsymbol{\Omega}^T \boldsymbol{\Omega}. \quad (33)$$

It is important to notice that $\boldsymbol{\beta}$ cannot be function of $\hat{\mathbf{z}}$, since its time derivative will give rise to \mathbf{z} .

4.3. Step 3: stability of the overall system

Now, we can state our main result in the following theorem.

Theorem 1. Consider the VTOL-UAV model (1), and let the desired trajectory $\mathbf{p}_d(t)$ and the controller gains k_{θ_1} and k_{θ_2} satisfy Assumption 1. Let the thrust input $\mathcal{T}(t)$ and the desired attitude $\mathbf{Q}_d(t)$ be given, respectively, by (6) and (7), with $\mathbf{F} \triangleq (\mu_1, \mu_2, \mu_3)^T$ given by (21) and (22). Let the torque input be as in (32) with the observer (28). Let the parameters $\boldsymbol{\psi}$ and $\boldsymbol{\beta}$, in (22) and (26) respectively, be given by

$$\dot{\boldsymbol{\psi}} = \lambda(\boldsymbol{\xi} - \boldsymbol{\psi}), \quad (34)$$

$$\boldsymbol{\beta} = -k_\beta \tilde{\mathbf{q}} + \frac{2\mathcal{T}}{k_q m} \mathbf{S}(\tilde{\mathbf{q}})^T \mathbf{R}(\mathbf{Q}) \mathbf{v}, \quad (35)$$

with $\lambda > 0$, $k_\beta > 0$, $\mathbf{v} = \hat{\mathbf{z}} + L_p \tilde{\boldsymbol{\xi}}$ and $\tilde{\mathbf{q}}$ defined in (14). Pick the control and observer gains as follows

$$L_p - L_v > \sigma_1, \quad L_v^3 > \sigma_2, \quad k_q k_\beta > \frac{\Lambda^2}{m^2} \left(\frac{1}{\sigma_1} + \frac{L_p^2}{\sigma_2} \right), \quad (36)$$

for some $\sigma_1 > 0$, $\sigma_2 > 0$, and Λ given in (24). Then, starting from any initial conditions, all signals are bounded and $\lim_{t \rightarrow \infty} \boldsymbol{\zeta}(t) = \mathbf{0}$, with $\boldsymbol{\zeta}(t)^T = (\mathbf{e}(t)^T, \tilde{\mathbf{v}}(t)^T, \tilde{\boldsymbol{\xi}}(t)^T, \tilde{\mathbf{z}}(t)^T, \tilde{\mathbf{q}}(t)^T, \tilde{\boldsymbol{\omega}}(t)^T)$.

Proof. First, it is easy to check that if the desired trajectory and the controller gains k_{θ_1} and k_{θ_2} satisfy Assumption 1, condition (8) is always satisfied, and hence it is always possible to extract the magnitude of the thrust and the desired attitude from (6) and (7) respectively for the VTOL vehicle. Consider the following Lyapunov function candidate

$$V = V_t + V_a. \quad (37)$$

Using (34) and (35), the time derivative of V evaluated along the system trajectories, in view of (20) and (33), is obtained as

$$\begin{aligned} \dot{V} = & -k_d \lambda (\boldsymbol{\xi} - \boldsymbol{\psi})^T (\boldsymbol{\xi} - \boldsymbol{\psi}) - (L_p - L_v) \tilde{\mathbf{z}}^T \tilde{\mathbf{z}} - L_v^3 \tilde{\boldsymbol{\xi}}^T \tilde{\boldsymbol{\xi}} - k_\Omega \boldsymbol{\Omega}^T \boldsymbol{\Omega} \\ & - k_q k_\beta \tilde{\mathbf{q}}^T \tilde{\mathbf{q}} + \frac{2\mathcal{T}}{m} \tilde{\mathbf{q}}^T \mathbf{S}(\tilde{\mathbf{q}})^T \mathbf{R}(\mathbf{Q}) (\tilde{\mathbf{z}} + L_p \tilde{\boldsymbol{\xi}}). \end{aligned} \quad (38)$$

Using the fact that $\|\mathbf{R}(\mathbf{Q})^T \mathbf{S}(\tilde{\mathbf{q}})\| \leq 1$ and $L_p > L_v$ from (36), an upper bound of \dot{V} can be obtained as

$$\begin{aligned} \dot{V} \leq & -k_d \lambda \|\boldsymbol{\xi} - \boldsymbol{\psi}\|^2 - (L_p - L_v - \sigma_1) \|\tilde{\mathbf{z}}\|^2 - k_\Omega \|\boldsymbol{\Omega}\|^2 \\ & - (L_v^3 - \sigma_2) \|\tilde{\boldsymbol{\xi}}\|^2 - \left(k_q k_\beta - \frac{\Lambda^2}{m^2} \left(\frac{1}{\sigma_1} + \frac{L_p^2}{\sigma_2} \right) \right) \|\tilde{\mathbf{q}}\|^2, \end{aligned} \quad (39)$$

where Λ is given in (24), and we have used the fact that for any real numbers a and b , we have $2ab \leq a^2/\sigma + \sigma b^2$, for some $\sigma > 0$. Therefore, \dot{V} is negative semi-definite if condition (36) is satisfied. Hence, we can conclude that \mathbf{z} , $\boldsymbol{\xi}$, $\boldsymbol{\psi}$, $\tilde{\mathbf{q}}$, $\boldsymbol{\Omega}$, $\tilde{\mathbf{z}}$ and $\tilde{\boldsymbol{\xi}}$ are bounded. Consequently, $\dot{\boldsymbol{\theta}}$, $\dot{\boldsymbol{\psi}}$, $\dot{\mathbf{z}}$, $\dot{\tilde{\mathbf{z}}}$ and \mathbf{v} are bounded. Also, we can see that $(\boldsymbol{\xi} - \boldsymbol{\psi})$ is bounded.

Since $\tilde{\mathbf{q}}$ and \mathbf{v} are bounded, we can see that $\boldsymbol{\beta}$ is bounded, and hence $\tilde{\boldsymbol{\omega}}$ is bounded from (26). Hence, we can conclude that $\tilde{\mathbf{q}}$ is bounded. In addition, we can easily verify that $\boldsymbol{\Omega}$ is bounded using the expressions of $\boldsymbol{\tau}$ in the closed loop dynamics (27). As a result, \dot{V} is bounded. Hence, invoking Barbalat lemma, we can conclude that $(\boldsymbol{\xi} - \boldsymbol{\psi}) \rightarrow 0$, $\tilde{\boldsymbol{\xi}} \rightarrow 0$, $\tilde{\mathbf{z}} \rightarrow 0$, $\boldsymbol{\Omega} \rightarrow 0$ and $\tilde{\mathbf{q}} \rightarrow 0$, and therefore we can conclude that $\mathbf{R}(\tilde{\mathbf{Q}}) \rightarrow \mathbf{I}_3$ and $\tilde{\boldsymbol{\eta}} \rightarrow \pm 1$.

Using the above results, we know that $\ddot{\boldsymbol{\xi}} - \ddot{\boldsymbol{\psi}} = \dot{\mathbf{z}} - \lambda(\boldsymbol{\xi} - \boldsymbol{\psi})$ is bounded, and since we have shown that $(\boldsymbol{\xi} - \boldsymbol{\psi}) \rightarrow 0$, we can conclude from Barbalat lemma that $(\ddot{\boldsymbol{\xi}} - \ddot{\boldsymbol{\psi}}) \rightarrow 0$. Consequently, we can conclude that $\dot{\boldsymbol{\xi}} = \mathbf{z} \rightarrow 0$, since $\dot{\boldsymbol{\psi}} = \lambda(\boldsymbol{\xi} - \boldsymbol{\psi}) \rightarrow 0$. Also, since

Table 1
Simulation parameters.

$\mathbf{p}(0) = (-2, 5, -1)$, $\mathbf{v}(0) = (0, 0, 0)$, $\mathbf{q}(0) = (0, 0, 0, 1)$,
$\boldsymbol{\omega}(0) = \boldsymbol{\theta}(0) = \dot{\boldsymbol{\theta}}(0) = \dot{\boldsymbol{\xi}}(0) = \mathbf{v}(0) = (0, 0, 0)$, $g = 9.8$,
$k_p = 0.3$, $k_d = 0.5$, $\lambda = 1$, $k_{\theta_1} = 1.5$, $k_{\theta_2} = 1.5$,
$k_\beta = 40$, $k_q = 40$, $k_\Omega = 30$, $L_p = 1.5$, $L_v = 0.8$.

\mathbf{z} and $\tilde{\mathbf{z}}$ converge to zero, it is clear that $\hat{\mathbf{z}}$ tends to zero, and with the limit of $\tilde{\boldsymbol{\xi}}$, one can conclude that $\mathbf{v} \rightarrow 0$, and consequently, $\boldsymbol{\beta} \rightarrow 0$ implying that $\tilde{\boldsymbol{\omega}} \rightarrow 0$.

Exploiting the above boundedness results, and since $\tilde{\mathbf{q}} \rightarrow 0$ and $(\boldsymbol{\xi} - \boldsymbol{\psi}) \rightarrow 0$, we can conclude from the translational error dynamics (16), with (19) and (14), that $\dot{\mathbf{z}} \rightarrow 0$ using the extended version of Barbalat lemma (See, for instance, Lemma 2 in Hua et al. (2009)). Hence, we conclude from (16) that $\boldsymbol{\xi} \rightarrow 0$ and consequently $\boldsymbol{\psi} \rightarrow 0$.

To show the convergence of \mathbf{e} and $\tilde{\mathbf{v}}$, we have to investigate the boundedness and asymptotic convergence to zero of the variables $\boldsymbol{\theta}$ and $\dot{\boldsymbol{\theta}}$. It can be seen that (22) can be rewritten as: $\dot{\boldsymbol{\theta}} = -k_{\theta_1} \tanh(\boldsymbol{\theta}) - k_{\theta_2} \tanh(\dot{\boldsymbol{\theta}}) + \boldsymbol{\chi}$, with $\boldsymbol{\chi} = k_p \boldsymbol{\xi} + k_d(\boldsymbol{\xi} - \boldsymbol{\psi})$. Using the above results, we can easily verify that $\boldsymbol{\chi}$ is bounded and tends to zero as t goes to infinity. Therefore, we can show that $\boldsymbol{\theta}$ and $\dot{\boldsymbol{\theta}}$ are bounded and converge asymptotically to zero, and as a result, $\mathbf{e} \rightarrow 0$ and $\tilde{\mathbf{v}} \rightarrow 0$ asymptotically.

To complete the proof, we must show that the input torque in (32) is bounded. Exploiting the above boundedness results, we can easily show that $\boldsymbol{\tau}$ is bounded if $\boldsymbol{\omega}_d$, $\dot{\boldsymbol{\omega}}_d$ and $\dot{\boldsymbol{\beta}}$ are bounded. By taking the time derivative of (35), we can show that $\frac{d}{dt}(\mathbf{S}(\tilde{\mathbf{q}})^T \mathbf{R}(\mathbf{Q}))$ is bounded if $\boldsymbol{\omega}$, $\dot{\boldsymbol{\omega}}$ are bounded, and since \mathbf{v} and $\dot{\mathbf{v}}$ are bounded, we know that $\dot{\boldsymbol{\beta}}$ is bounded if $\dot{\mathcal{T}}$ and $\dot{\boldsymbol{\omega}}_d$ are bounded. It is important to note from the time derivative of (35) that $\dot{\boldsymbol{\beta}}$ used in (32) is completely known, since $\tilde{\boldsymbol{\omega}}$ and $\dot{\mathbf{v}}$ are available from (13) and (28) respectively. As a result, we conclude that $\boldsymbol{\tau}$ is bounded if $\dot{\mathcal{T}}$, $\boldsymbol{\omega}_d$ and $\dot{\boldsymbol{\omega}}_d$ are bounded.

Using the above boundedness results, it is clear that $\dot{\mathbf{F}}$ and $\ddot{\mathbf{F}}$ are bounded, and $\lim_{t \rightarrow \infty} \mathbf{F} = \dot{\mathbf{p}}_d$, $\lim_{t \rightarrow \infty} \dot{\mathbf{F}} = \mathbf{p}_d^{(3)}$ and $\lim_{t \rightarrow \infty} \ddot{\mathbf{F}} = \mathbf{p}_d^{(4)}$, where $\mathbf{p}_d^{(3)}$ and $\mathbf{p}_d^{(4)}$ are, respectively, the third and fourth derivatives of the desired trajectory, which are assumed to be bounded. Hence, using (6), (9) and (25), with (10), (A.2), (A.3) and Assumption 1, we can conclude that $\dot{\mathcal{T}}$, $\boldsymbol{\omega}_d$ and $\dot{\boldsymbol{\omega}}_d$ are bounded, and this ends the proof. \square

5. Simulation results

Simulation results are presented to illustrate the effectiveness of the proposed control scheme. Using SIMULINK, we consider a VTOL UAV modeled as a rigid body of mass $m = 3$ kg and with inertia matrix $\mathbf{I}_f = \text{diag}(\text{col}(0.13, 0.13, 0.04))$ kg m². The simulation parameters are illustrated in Table 1. The desired trajectory is given by $\mathbf{p}_d(t)^T = (10 \cos(0.1t + 2), 10 \sin(0.1t + 2.4), t)$ m. Note that the controller gains are selected to satisfy case (c) of Assumption 1 and condition (36). The obtained results are illustrated in Figs. 2–6.

Figs. 2 and 3 illustrate the three components of the position and velocity tracking errors. Fig. 4 shows the attitude tracking error and Fig. 5 illustrates the desired and actual angular velocity of the aircraft. It is clear from these figures that asymptotic convergence to zero is guaranteed after few seconds. To illustrate the vehicle's position tracking, a 3-D plot of the vehicle's position with the desired trajectory is given in Fig. 6, as well as the projections of the curves in the different planes.

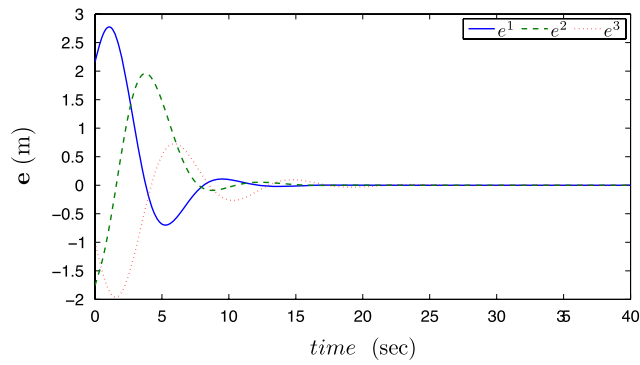


Fig. 2. Position tracking error, with $e = (e^1, e^2, e^3)^T$.

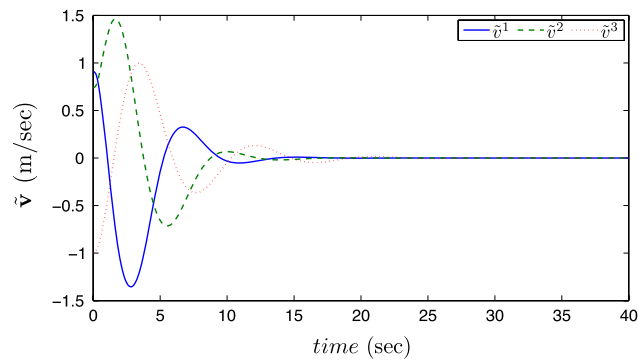


Fig. 3. Velocity tracking error, with $\tilde{v} = (\tilde{v}^1, \tilde{v}^2, \tilde{v}^3)^T$.

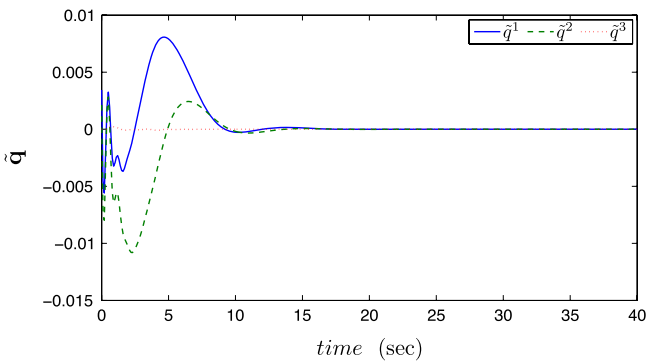


Fig. 4. Attitude tracking error, with $\tilde{q} = (\tilde{q}^1, \tilde{q}^2, \tilde{q}^3)^T$.

6. Concluding remarks

We addressed the trajectory tracking problem of a class of under-actuated systems, VTOL-UAVs, without linear-velocity measurements. A separate translational and rotational control design was presented, and global asymptotic stability of the overall closed loop system was shown. At the first stage of the control design, the requirement of the linear velocity has been obviated with the introduction of new control variables reshaping the desired trajectory during the transient. In the second stage of the control design, a nonlinear observer has been derived and used to design a linear-velocity-free control torque guaranteeing the tracking of the desired attitude derived at the first stage of the control design.

To the best of our knowledge, the proposed linear-velocity-free control scheme is a new result providing global asymptotic tracking for the class of under-actuated systems under consideration. Furthermore, the proposed control strategy can be easily modified to solve the trajectory tracking problem of VTOL-UAVs in the case where the linear-velocity is available for feedback, and global results can be shown. This result constitutes on its own right an

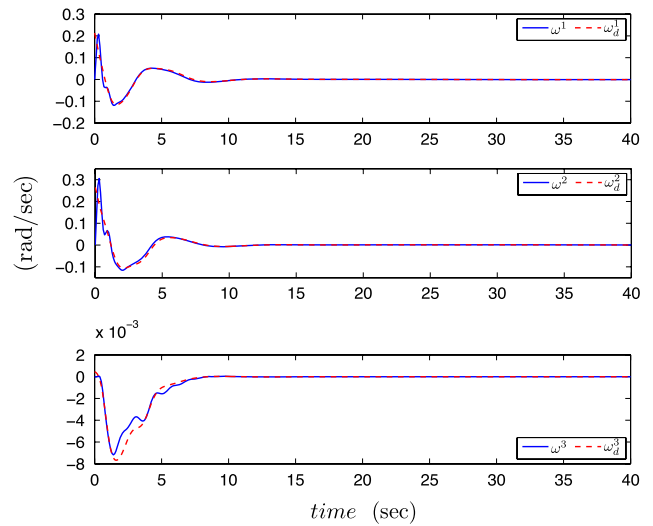


Fig. 5. Elements of the aircraft angular velocity and the desired angular velocity vectors, with $\omega^T = (\omega^1, \omega^2, \omega^3)$ and $\omega_d^T = (\omega_d^1, \omega_d^2, \omega_d^3)$.

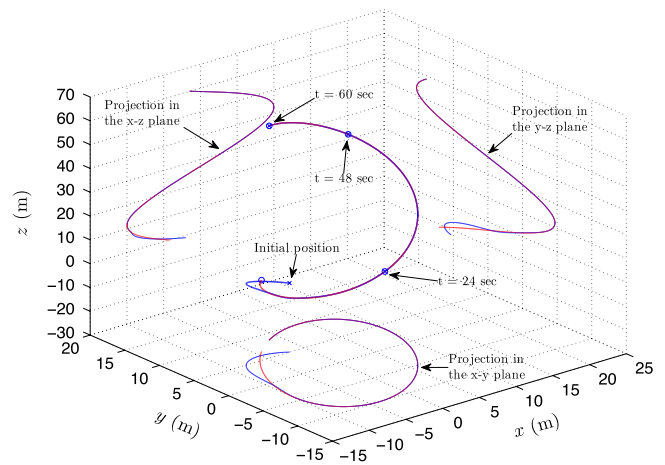


Fig. 6. 3D plot of the VTOL vehicle trajectory (blue) with the desired trajectory (red). (For interpretation of the references to colour in this figure legend, the reader is referred to the web version of this article.)

interesting contribution since global results are difficult to obtain for this class of under-actuated systems. In the case where the linear velocity is available, a global result has been obtained in [Frazzoli et al. \(2000\)](#) for the trajectory tracking problem, where the control is guaranteed to be smooth provided that the rotation angle of the attitude error is different from $\pi/2$. Also, the thrust input is defined as a solution to a second order differential equation. The authors in [Frazzoli et al. \(2000\)](#), first determine an optimal desired thrust input and desired orientation, then using the backstepping procedure, a thrust and input torque are determined. A conceptually similar approach is considered in [Hamel et al. \(2002\)](#) to solve the stabilization problem. The main difference between the proposed approach and the work of [Frazzoli et al. \(2000\)](#) and [Hamel et al. \(2002\)](#), besides the non-availability of the linear velocity, is the adopted singularity-free attitude extraction method (in terms of unit-quaternion) as well as the *a priori* boundedness of the virtual translational control input and the system's thrust.

Acknowledgements

This work was supported by the Natural Sciences and Engineering Research Council of Canada (NSERC).

Appendix

We derive in the following the expressions of the variables Ψ_1 and Ψ_2 in Eq. (25). From (9), we can write $\dot{\omega}_d = \Xi(\mathbf{F})\dot{\mathbf{F}} + \Xi(\mathbf{F})\ddot{\mathbf{F}}$, where $\Xi(\mathbf{F})$ can be directly obtained from $\dot{\mathbf{F}}$ with $\gamma_1 = \frac{1}{\gamma_1}(\mu_1 \quad \mu_2 \quad -(g - \mu_3))\dot{\mathbf{F}}$. In view of the design (21), we have

$$\begin{aligned}\dot{\mathbf{F}} &= \mathbf{p}_d^{(3)} - k_{\theta_1}h(\boldsymbol{\theta})\dot{\boldsymbol{\theta}} - k_{\theta_2}h(\dot{\boldsymbol{\theta}})\ddot{\boldsymbol{\theta}} \\ \ddot{\mathbf{F}} &= \mathbf{p}_d^{(4)} - k_{\theta_1}\bar{h}(\boldsymbol{\theta})\ddot{\boldsymbol{\theta}} - (k_{\theta_1}h(\boldsymbol{\theta}) + k_{\theta_2}\bar{h}(\dot{\boldsymbol{\theta}}))\ddot{\boldsymbol{\theta}} \\ &\quad - k_{\theta_2}h(\dot{\boldsymbol{\theta}})\{(k_d + k_p)\mathbf{z} - k_d\dot{\boldsymbol{\psi}} - k_{\theta_1}h(\boldsymbol{\theta})\dot{\boldsymbol{\theta}} - k_{\theta_2}h(\dot{\boldsymbol{\theta}})\ddot{\boldsymbol{\theta}}\}\end{aligned}\quad (\text{A.1})$$

where $\mathbf{p}_d^{(3)}$ and $\mathbf{p}_d^{(4)}$ are, respectively, the third and fourth derivatives of the desired trajectory, and for $\mathbf{u} = (u_1, u_2, u_3)^T \in \mathbb{R}^3$, we have defined $h(\mathbf{u}) = \text{diag}(v_1^1, v_1^2, v_1^3)$ and $\bar{h}(\mathbf{u}) = \text{diag}(v_2^1, v_2^2, v_2^3)$, with $v_i^1 = (1 - \tanh^2(u_i))$ and $v_i^2 = (-2\dot{u}_i(1 - \tanh^2(u_i)) \tanh(u_i))$, for $i = 1, 2, 3$, and “diag” is the diagonal matrix operator. Hence we can rewrite $\dot{\omega}_d$ as in (25) with

$$\begin{aligned}\Psi_1 &= \Xi(\mathbf{F})\dot{\mathbf{F}} + \Xi(\mathbf{F})\{\mathbf{p}_d^{(4)} - k_{\theta_1}\bar{h}(\boldsymbol{\theta})\ddot{\boldsymbol{\theta}} \\ &\quad - k_{\theta_2}h(\dot{\boldsymbol{\theta}})(-k_d\dot{\boldsymbol{\psi}} - k_{\theta_1}h(\boldsymbol{\theta})\dot{\boldsymbol{\theta}} - k_{\theta_2}h(\dot{\boldsymbol{\theta}})\ddot{\boldsymbol{\theta}}) \\ &\quad - (k_{\theta_1}h(\boldsymbol{\theta}) + k_{\theta_2}\bar{h}(\dot{\boldsymbol{\theta}}))\ddot{\boldsymbol{\theta}}\},\end{aligned}\quad (\text{A.2})$$

$$\Psi_2 = k_{\theta_2}(k_p + k_d)\Xi(\mathbf{F})h(\dot{\boldsymbol{\theta}}).\quad (\text{A.3})$$

References

- Abdessameud, A., & Tayebi, A. (2009). Formation control of VTOL UAVs. In *Proceedings of the 48th IEEE conference on decision and control* (pp. 3454–3459).
- Aguiar, A. P., & Hespanha, J. P. (2007). Trajectory-tracking and path-following of underactuated autonomous vehicles with parametric modeling uncertainty. *IEEE Transactions on Automatic Control*, 52(8), 1362–1379.
- Benzemrane, K., Santosuosso, G. L., & Damm, G. (2007). Unmanned aerial vehicle speed estimation via nonlinear adaptive observers. In *Proceedings of the American control conference* (pp. 958–990).
- Chevron, T., Hamel, T., Mahony, R., & Baldwin, G. (2007). Robust nonlinear fusion of inertial and visual data for position, velocity and attitude estimation of UAV. In *Proceedings of the IEEE international conference on robotics and automation* (pp. 2010–2016).
- Do, K. D., Jiang, Z. P., & Pan, J. (2003). On global tracking control of a VTOL aircraft without velocity measurements. *IEEE Transactions on Automatic Control*, 48(12), 2212–2217.
- Frazzoli, E., Dahleh, M. A., & Feron, E. (2000). Trajectory tracking control design for autonomous helicopters using a backstepping algorithm. In *Proceedings of the American control conference* (pp. 4102–4107).
- Hamel, T., Mahony, R., Lozano, R., & Ostrowski, J. (2002). Dynamic modelling and configuration stabilization for an x4-flyer. In *Proceedings of the 15th IFAC world congress*.
- Hua, M., Hamel, T., Morin, P., & Samson, C. (2009). A control approach for thrust-propelled underactuated vehicles and its application to VTOL drones. *IEEE Transactions on Automatic Control*, 54(8), 1837–1853.
- Kaminer, I., Pascoal, A., Hallberg, E., & Silvestre, C. (1998). Trajectory tracking controllers for autonomous vehicles: an integrated approach to guidance and control. *Journal of Guidance and Control Dynamics*, 21(1), 29–38.
- Kendoul, F., Lara, D., Fantoni, I., & Lozano, R. (2006). Nonlinear control for systems with bounded inputs: real-time embedded control applied to UAVs. In *Proceedings of the 45th IEEE conference on decision & control* (pp. 5888–5893).
- Koo, T., & Sastry, S. (1998). Output tracking control design of a helicopter model based on approximate linearization. In *Proceedings of the 37th IEEE conference of decision and control* (pp. 3635–3640).
- Madani, T., & Benallegue, A. (2007). Backstepping control with exact 2-sliding Mode estimation for a quadrotor unmanned aerial vehicle. In *Proceedings of the 2007 IEEE/RSJ international conference on intelligent robots and systems* (pp. 141–146).
- Pflimlin, J. M., Soueres, P., & Hamel, T. (2007). Position control of a ducted fan VTOL UAV in crosswind. *International Journal of Control*, 80(5), 666–683.
- Roberts, A., & Tayebi, A. (2009). Adaptive position tracking with external disturbance estimation for a VTOL-UAV. In *Proceedings of the 48th IEEE conference on decision and control* (pp. 5233–5238).
- Rondon, E., Salazar, S., Escareno, J., & Lozano, R. (2010). Vision-based position control of a two-rotor VTOL miniUAV. *Journal of Intelligent and Robotic Systems*, 57, 49–64.
- Shuster, M. D. (1993). A survey of attitude representations. *Journal of Astronautical Sciences*, 41(4), 439–517.
- Tayebi, A. (2008). Unit quaternion based output feedback for the attitude tracking problem. *IEEE Transactions on Automatic Control*, 53(6), 1516–1520.
- Wen, J. T.-Y., & Kreutz-Delgado, K. (1991). The attitude control problem. *IEEE Transactions on Automatic Control*, 36(10), 1148–1162.



Abdelkader Abdessameud received his Engineer degree in Electrical Engineering from Institut National d'Electricité et d'Electronique, INELEC, Algeria, in 1995, and his M.Sc. (Magister) in robotics from Ecole Militaire Polytechnique de Bordj-El-Bahri, Algeria, in 1999. From 2001 to 2007, he served as a Lecturer (Maître assistant chargé de cours) and Research Assistant at département d'Automatisation des procédés industriels at the University of Boumerdes, Algeria. He is currently a Ph.D. student in the department of Electrical and Computer Engineering at the University of Western Ontario, Canada. His research interest focuses on the control of autonomous aerial vehicles, attitude synchronization and cooperative control of multi-vehicle systems.



Abdelhamid Tayebi received his B.Sc. in Electrical Engineering from Ecole Nationale Polytechnique d'Alger, Algeria in 1992, his M.Sc. (DEA) in robotics from Université Pierre & Marie Curie, Paris, France in 1993, and his Ph.D. in Robotics and Automatic Control from Université de Picardie Jules Verne, France in December 1997. He joined the department of Electrical Engineering at Lakehead University in December 1999 where he is presently a Professor. He is a Senior Member of IEEE and serves as an Associate Editor for IEEE Transactions on Systems, Man, and Cybernetics – Part B; Control Engineering Practice and IEEE CSS Conference Editorial Board. He is the founder and Director of the Automatic Control Laboratory at Lakehead University. His research interests are mainly related to linear and nonlinear control theory including adaptive control, robust control and iterative learning control, with applications to robot manipulators and aerial vehicles.